



# Micro-flame ionization detector with a novel structure for portable gas chromatograph

Jianwei Wang, Hua Wang, Chunfeng Duan, Yafeng Guan\*

Department of Instrumentation & Analytical Chemistry, Key Lab of Separation Science for Analytical Chemistry, Dalian Institute of Chemical Physics, Chinese Academy of Sciences, Dalian 116023, China

## ARTICLE INFO

### Article history:

Received 12 April 2010  
Received in revised form 1 June 2010  
Accepted 2 June 2010  
Available online 11 June 2010

### Keywords:

Micro-flame ionization detector  
Coaxial gas flow  
Ionization efficiency  
Portable gas chromatograph

## ABSTRACT

A micro-flame ionization detector ( $\mu$ -FID) for portable gas chromatograph (GC) based on conventional mechanical fabrication techniques was developed and evaluated. Structure was redesigned and dimensions were optimized for best performance. Air is introduced from upper part of the detector, flowing downwards into the burning chamber along a narrow round gap between the collection electrode and the inner wall of the detector body, forming a uniform flow field around the burning jet. The lowest detection limit of the  $\mu$ -FID was  $5 \times 10^{-13}$  g/s for n-decane, with a linear response range of five orders of magnitude. The consumption of gases is only 10 ml/min for hydrogen, and 120 ml/min for air, that is about 1/3 of the gases required for conventional FIDs. A comparative study between the  $\mu$ -FID and commercial FID was also performed that proved the advantages of the  $\mu$ -FID. The  $\mu$ -FID is simple in structure, low heating power, and low consumption of gases that not only decrease the cost of running, but also increase the portability of GC for filed applications.

© 2010 Elsevier B.V. All rights reserved.

## 1. Introduction

The portable gas chromatograph (GC), also named micro GC, is an attractive analytical instrument because of its practical applications in numerous fields such as *in situ* environmental monitoring, chemical industry, medicine, emergency detection and so on [1,2]. As one of the major components in GC, the detector and its supporting conditions have great impacts on the design and the overall performance of the portable GC. Miniature detectors are attractive for portable gas chromatographs because of their low gas consumption, very small in size, low power requirements for operation and heating, and reasonable sensitivity as compared with that of conventional ones. Many miniature detectors have been designed for portable GC, including solid state thermal conductivity detector ( $\mu$ -TCD or SSD) [3–5], photoionization detector (PID) [6,7], arrays of surface acoustic wave (SAW) sensor [8–10] and so on. The miniature TCD or SSD, has been widely used in micro GCs [3–5]. However, the use of SSD requires high purity helium or hydrogen as carrier gas since it is sensitive to all permanent gases and contaminants. In addition, detection of sub-ppm or even ppb level concentration of contaminants, typically in environmental or food samples, is out of the capability of GCs equipped with SSD.

The PID is another detector adopted by portable GC [6,7]. The PID is usually suitable to detect halogen compounds and aromatic hydrocarbons because of its selective and sensitive responses. The flame ionization detector (FID), on the other hand, is a universal detector for detection of trace levels of organic compounds because of its high sensitivity, wide linear range, general responses to most of organics and lack of response to almost all permanent and inert gases except methane [11].

Efforts have been made to miniaturize FID detectors for portable GC. Zimmermann et al. presented a sandwich-constructed micro-FID ( $\mu$ -FID) based on three-dimensional micro-electro-mechanical systems (MEMS) technology [12,13]. Kevin and co-workers constructed a  $\mu$ -FID with counter-flowing stream of gas by quartz and stainless steel tubes [14–16]. Although these attempts simplified the structure of the detector and reduced its volume, the sensitivity was lower than that of the conventional FID. In this study, we reported a high sensitive  $\mu$ -FID by using conventional mechanical fabrication techniques. One distinct design was developed and described in detail. The structure and parameters of the  $\mu$ -FID were optimized, and the performance of the detector was evaluated.

## 2. Theory

The ionization of organic compounds burned in an oxyhydrogen flame was generally considered as the physical basis of common FIDs. First, when the materials eluting from the column enter the flame, a group of single-carbon species are generated through

\* Corresponding author. Tel.: +86 411 84379590; fax: +86 411 84379570.  
E-mail addresses: [guan\\_yafeng@yahoo.com.cn](mailto:guan_yafeng@yahoo.com.cn), [guanyafeng@dicp.ac.cn](mailto:guanyafeng@dicp.ac.cn), [kfguan@mail.dlptt.ln.cn](mailto:kfguan@mail.dlptt.ln.cn) (Y. Guan).

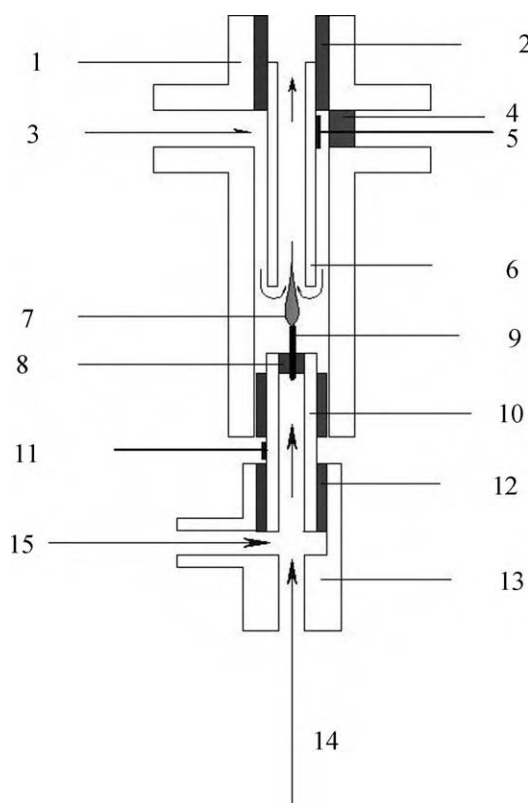
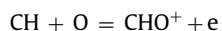
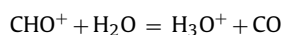


**Fig. 1.** Schematic diagram of the micro-flame ionization detector. (1) Cross union; (2) PTFE tube; (3) air; (4) PTFE ferrule; (5) signal cable; (6) collector electrode; (7) flame; (8) heat-resistant inorganic glue; (9) jet tip; (10) stainless steel tube; (11) polarization voltage; (12) PTFE tube; (13) tri-port union; (14) carrier gas; (15) makeup gas.

degradation reactions in the hydrogen-rich region of the flame. These single-carbon species include CH, CH<sub>2</sub>, and CH<sub>3</sub> radicals. Next, as these radicals move into the zone containing oxygen, a chemi-ionization reaction takes place:



Then, the CHO<sup>+</sup> ions react rapidly with water to generate hydroxonium ions. The process can be expressed as follows:



Finally, the H<sub>3</sub>O<sup>+</sup> ions are collected by the collector electrode in the detector under the drive of a polarization voltage, producing an increase in current. Thus, the ionization current is proportional to the number of carbon atoms present, which is the basis of quantification of FID as a GC detector. The ionization efficiency of the organic compounds is about 1/10<sup>6</sup> [11].

### 3. Experimental

The basic structure of the μ-FID is shown in Fig. 1. The size of the main body of the detector is 50 mm × Ø 10 mm. The collection electrode (5 in Fig. 1), a stainless steel tube (2.5 mm I.D., 3.2 mm O.D.), is placed in the center of a stainless steel cross (1 in Fig. 1). A PTFE ring (2 in Fig. 1) is then inserted to fix and insulate the collection electrode, and to seal auxiliary gas of air. The jet tip of μ-FID, a piece of fused silica or stainless steel capillary (8 mm in length), is adhered to a stainless steel tube (0.8 mm I.D., 1.6 mm O.D., 9 in Fig. 1) with heat-resistant inorganic glue (7 in Fig. 1), and then fixed into the cross with PTFE tube or Vespel ferrule. The air (3 in Fig. 1) is introduced into the burning chamber through the left port of the cross.

The air flow pattern in the detector proposed here was essential to the sensitivity of the detector. As shown in Fig. 1, the introduced air flows downwards along the gap between the detector shell and the collection electrode before entering into the burning chamber of the μ-FID. As the air flows against the bottom of the chamber, it changes the flow direction to horizontal (90°) and then opposite (180°), and then along the inner hole of the collection electrode and escapes from the outlet of the electrode. In the zone around the flame, air flows around the flame. This design is beneficial to the air flow stability around the flame, resulting in low noise levels and improved high signal-to-noise ratio. A higher polarization voltage (600–800 V) is then applied between the jet and the collector electrode. An amplifier is connected to the collection electrode of the μ-FID through the right port of the cross union. The whole μ-FID body is installed on a model HP4890 GC instrument (Hewlett Packard Corporation, U.S.) with a home-made adapter. A heater of 20 W and the temperature sensor on the original heating port were installed into the adaptor to heat the μ-FID. They were connected with the instrument in replace of the original heater.

The amplifier used for evaluation of the μ-FID is from another GC instrument (GC9790, Fuli Analytical Instruments Ltd., China). The signals after amplification are recorded and processed by a model of N2000 chromatographic station (Zhida IT Company Ltd., China). Hydrogen obtained from a hydrogen generator was further purified by an oxygen-water trap. Typical experiments employ hydrogen as the carrier gas and the makeup gas. The separation column is OV-1 megabore quartz capillary column (30 m × 0.53 mm × 1.0 μm, Kefen, Scien-Tech Instruments Inc., Dalian, China).

## 4. Results and discussion

### 4.1. Coaxial flow of air around the jet tip

In our early study of the FID, it was observed that the flow pattern of the air around the jet tip influenced the noise level of the FID detector. A porous stainless steel plate was placed above the outlet area of air to disperse and stabilize the air flow at the bottom of a conventional FID. However, the improvement on noise level was rather weak as long as the air flow was stable. We designed the detector according to this idea and showed the structure of the design in Fig. 1, where a coaxial flow of air was generated through the gap between the electrode of collector and the inner wall of the detector body. In this case, the low noise level was achieved and the structure of the μ-FID was simplified meanwhile.

The μ-FID proposed in this work has different structures from other commercial FIDs. To achieve best performance, the main components of the μ-FID, including the jet tip and the collector electrode, some structural parameters such as the distance between jet tip and collector electrode, gas flow rate, and the polarization voltage were studied in detail.

### 4.2. Material and inner diameter of jet tip

The jet tip is one of the key parts to determine the final performance of the μ-FID detector. In this study, four fused silica capillaries of different diameters and a stainless steel capillary were employed as jet tips and were compared. The capillaries (8 in Fig. 1) were first stuck into a stainless steel tube of 0.8 mm I.D. and 1.6 mm O.D. (9 in Fig. 1) with inorganic glue (7 in Fig. 1). After the glue dried thoroughly, the tip, together with the stainless steel tube, was then installed into the cross union (1 in Fig. 1) for testing.

As shown in Table 1, for the jet tips of fused silica capillaries, the response increased as the inner diameter decreased. A possible explanation was that the smaller the inner diameter, the longer and thinner of the flame, which in turn benefit the air diffusion into

**Table 1**  
Effect of material and inner diameter of the capillary used as the jet tip on the response of the detector.

No.	Material	Inner diameter ( $\mu\text{m}$ )	Outer diameter ( $\mu\text{m}$ )	Response ( $\mu\text{V} \times \text{S}$ , $n=3$ )
01	Quartz	75	365	1857
02	Quartz	100	365	1955
03	Quartz	150	450	625
04	Quartz	200	320	Not found
05	Stainless steel	180	400	13,168

the centre of the flame, resulting in an increase in the ionization efficiency [17]. Moreover, the effect of jet materials on the detector response was even greater than that of inner diameters. The stainless steel capillary jet of 180  $\mu\text{m}$  I.D. and 400  $\mu\text{m}$  O.D. exhibited exceptionally higher response than that of quartz capillary jets. According to a report [18], carbon atoms in a hydrocarbon molecule were quantitatively converted to  $\cdot\text{CH}_3$  radicals in the lower part of the flame where a flux of the mobile hydrogen atoms was formed by diffusion inward from the combustion zone, and these processes were completed extremely fast in the flame at 600–650 °C. Since stainless steel has better thermal conductivity than quartz, the jet tip made of stainless steel made it easier to maintain an appropriate temperature to form  $\cdot\text{CH}_3$  radical in the lower part of the flame.

#### 4.3. Length of collector electrode

Four stainless steel tubes with the same inner (2.5 mm) and outer diameters (3.2 mm) were used to evaluate the effect of collector length. Their lengths were 17, 21, 24 and 27 mm, respectively. The stainless steel tubes were installed into the cross as the collector electrode (5 in Fig. 1) and tested by the same sample under the same experimental conditions. It was found that the length of the collector electrode had a little effect on the response of the  $\mu$ -FID within the experimental conditions. Therefore, the 21 mm-long collector electrode was chosen in the following experiments.

#### 4.4. Distance between the jet tip and the collector electrode

The distance between the jet tip and the collector was adjusted by changing the fixed position of the stainless steel tube (9 in Fig. 1) below the jet tip. The “negative” distance was defined as the relative distance that the jet tip extended into the collector electrode. The tested range of the distance was from –3.0 to 3.0 mm with steps of 0.5 mm at a polarization voltage of 150 V. The highest response

was obtained at the distance of 0–1 mm. This might because the diffusion efficiency of air into the center of the flame could decrease markedly when the distance exceeded 1 mm, since the linear flow velocity of air around the tip was slower outside the collector than that inside the collector. Furthermore, the temperature of the flame was lower when the flame was burning inside the collector than that outside the collector because of better heat dissipation generated by faster flow velocity of air and metal collector.

#### 4.5. Gas flow rate

In order to maximize the  $\mu$ -FID detector sensitivity, the burning in the flame should be as thoroughly as possible. The gas flow rate can directly influence the burning efficiency. The total hydrogen flow rate was the sum of makeup gas and carrier gas in the experiment. When studying the effect of the total hydrogen flow rate, the carrier gas ( $\text{H}_2$ ) and air were set at 6 and 180 ml/min, respectively, while changing the makeup gas ( $\text{H}_2$ ) from 0 to 8 ml/min. The best signal-to-noise ratio was obtained when the total hydrogen flow rate reached 10 ml/min. So the total hydrogen flow rate was set at 10 ml/min, and the flow rate of air was changed the flow rate of air from 60 to 160 ml/min with a step of 20 ml/min. The best signal-to-noise ratio was reached at a flow rate of 120 ml/min of air, namely the air-to-hydrogen ratio of 12:1. Therefore, in the following experiments, the flow rates of the total hydrogen and air were set at 10 and 120 ml/min, respectively.

#### 4.6. Polarization voltage

For a conventional FID, the voltage between the jet tip and the collector electrode is between 25 and 300 V to collect the ions/electrons effectively. When the polarization voltage is above a certain level, there is no improvement on signal-to-noise ratio [11]. Generally speaking, a voltage of 150–250 V is sufficient, higher

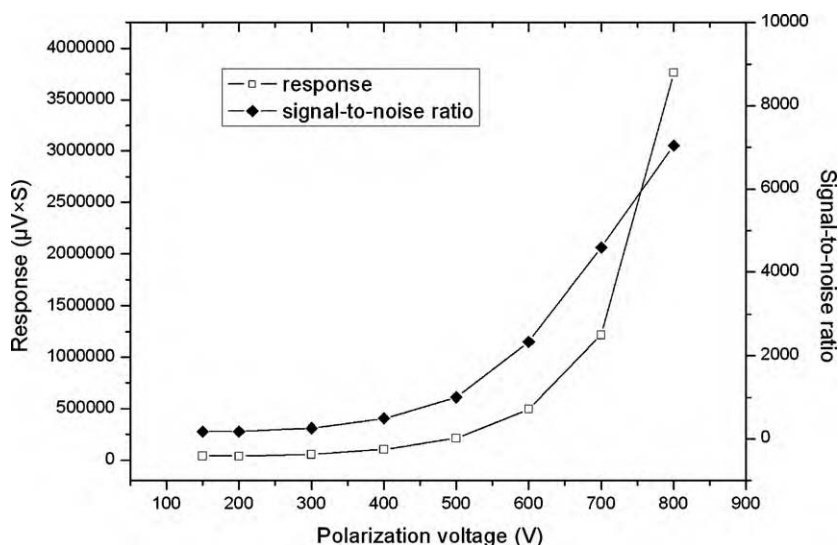


**Fig. 2.** Effect of polarization voltage on the response and signal-to-noise ratio of the  $\mu$ -FID proposed.

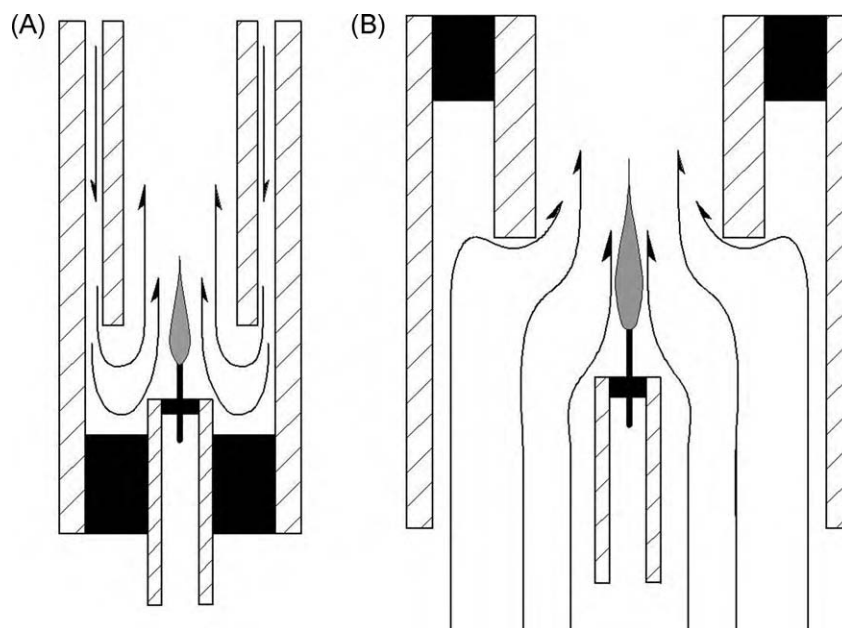


Fig. 3. Gas flow pattern in  $\mu$ -FID proposed in this work (A) and conventional FID (B).

polarization voltage does not lead to higher response. However, for the  $\mu$ -FID designed in this work, we observed an interesting phenomenon. When the polarization voltage increased gradually from 150 to 800 V, the response increased linearly below 400 V (Fig. 2), and then rapidly increased once the polarization voltage exceeded 500 V. Although the baseline noise increased with increasing voltage as well, the raise of signal was much higher. The signal-to-noise ratio at different polarization voltages was also shown in Fig. 2. The data in Fig. 2 proved that the signal-to-noise ratio was improved as the voltage increased. Compared to the response at polarization voltages of 150 V, the signal-to-noise ratio obtained at 800 V improved drastically. These findings suggested that the sensitivity of the  $\mu$ -FID could be improved greatly by increasing the polarization voltage.

When the polarization voltage increased from 150 to 800 V, the level of baseline increased about 72 mV for  $\mu$ -FID, and 400 mV for conventional FID with the same jet tip (9 in Fig. 1) which was installed by a home-made adapter. This suggested that in the  $\mu$ -FID, the leakage current is much smaller than that in the conventional FID under high polarization voltages; and the structure design of the  $\mu$ -FID was essential to obtain this feature.

The different behavior of the detector response on the polarization voltage between the conventional FID and the  $\mu$ -FID proposed was surprising. Except for the jet tip component, the major difference between the two types of detectors was the gas flow pattern and stability around the jet tip, and the distance between the tip and the electrode. As shown in Fig. 3B, for the conventional FID, the air flows from the bottom of the tip and parallel to the axis

of the flame; while in the  $\mu$ -FID (Fig. 3A), a coaxial flow of air is generated along a narrow round gap between the collection electrode and the inner wall of the detector body. The coaxial flow of air flows downward to the bottom of the chamber and then turned back to the hollow collector. Since the jet tip is located in the center part of air flow and the air flow in the center part is extremely stable, the noise generated from the stable air flow is then very low compared with that in conventional FID. The rather short distance between the tip and the electrode allows application of high polarization voltage between them, resulting in an increase in ionization efficiency and/or fast separation for electrons and positive charges. These results showed that the novel structure of the  $\mu$ -FID together with the high polarization voltage yield the high sensitivity of the detector.

#### 4.7. Performance of the $\mu$ -FID

In order to characterize the analytical performance of the  $\mu$ -FID, the responses of the  $\mu$ -FID to different samples at series of concentrations were carefully examined. The detector was operated at a polarization voltage of 800 V and a temperature of 180 °C. The column oven temperature was 90 °C. It was found that the response of  $\mu$ -FID was linear with the concentration of n-decane from 0.05 to 5000 mg/l. The equation of the calibration curve was  $A = 15263.5C + 1.533$ , with a correlation coefficient ( $R^2$ ) of 0.9922 (here A stands for the peak area, C stands for the concentration). The limit of detection (LOD) calculated as  $3N/S$  was  $5 \times 10^{-13}$  g/s (here N was the point-to-point noise and S ( $\mu$ V s/g) was the sensitivity).

**Table 2**  
Results of response reproducibility of the  $\mu$ -FID towards different compounds.

Peak	Compound	Boiling point (°C)	Concentration (mg/l)	Peak area <sup>a</sup> ( $\mu$ V $\times$ S)	RSD (%)
A	n-Decane	174	54.5	2,939,831	0.9
B	n-Undecane	196	50.0	2,743,150	1.4
C	n-Dodecane	216	49.5	2,766,409	1.5
D	n-Tridecane	230	50.6	2,840,046	1.4
E	n-Tetradecane	251	49.0	2,740,151	2.8
F	n-Pentadecane	268	50.0	2,966,805	1.8
G	n-Hexadecane	280	54.5	3,190,366	1.1
H	Cyclohexane	81	Balance		

<sup>a</sup> Average of responses for five days. Each day three injections were carried out.

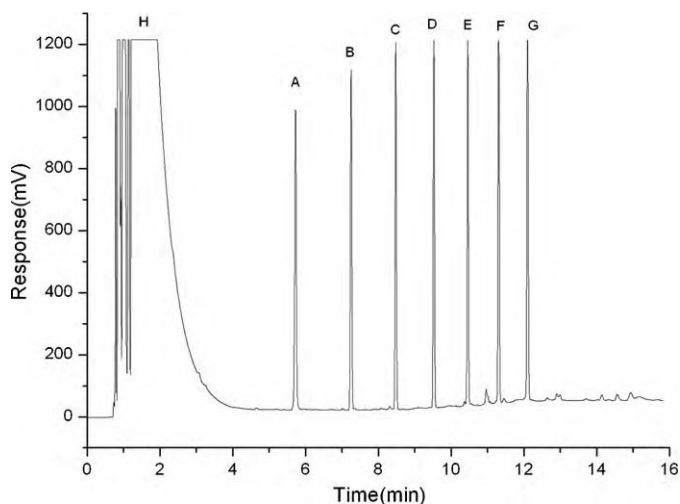


**Fig. 4.** Chromatogram of the test mixture. (A) n-Decane; (B) n-undecane; (C) n-dodecane; (D) n-tridecane; (E) n-tetradecane; (F) n-pentadecane; (G) n-hexadecane; (H) cyclohexane.

To investigate the reproducibility of the  $\mu$ -FID, a test mixture containing compounds with different boiling points was prepared. To ensure complete evaporation of the components especially those with relatively high boiling points, the temperature of the inlet was set to 300 °C. The GC temperature program was 80 °C initially for 2 min, then up to 200 °C at 15 °C/min. The  $\mu$ -FID was heated to 220 °C. The other experiment conditions were the same as those mentioned above. A typical chromatogram is shown in Fig. 4. The average response and RSD were calculated by analyzing the same samples in five days, with three injections in parallel each day. The results are listed in Table 2. It was found that the RSD of the  $\mu$ -FID responses for C<sub>10</sub>–C<sub>16</sub> were below 3%.

For a conventional FID, the degradation of hydrocarbons in the FID flame is not pyrolytic. Because of the attack by hydrogen atoms, a portion of hydrocarbons is converted to  $\bullet$ CH<sub>3</sub> radical. This leads to the phenomenon that hydrocarbons give responses in proportion to the number of carbon atoms contained, namely so called “the rule of equal response per carbon” [18,19]. Considering that the  $\mu$ -FID proposed here exhibited some different characteristics such as the structure and operation conditions, it is necessary to check whether the rule of equal response per carbon was effective for the  $\mu$ -FID. As shown in Fig. 5, the responses were in proportion to the number of carbon atoms in the range from 10 to 16, indicating that

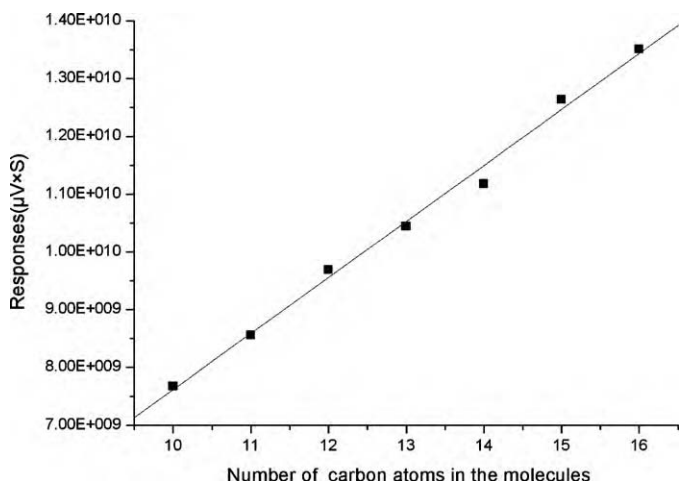


**Fig. 5.** Response of the  $\mu$ -FID to the number of carbon atoms in molecules.

**Table 3**

Comparison of the responses between  $\mu$ -FID and conventional FIDs.

	Peak height ( $\mu$ V)	Peak area ( $\mu$ V $\times$ s)	Noise ( $\mu$ V)	Signal-to-noise ratio (p-p)
$\mu$ -FID	11,029	125,707	100	110.3
Commercial FID	1055	12,436	35	35.1

the mechanism of the  $\mu$ -FID under high polarization voltage was still the same as that of conventional FID.

The sensitivity of the  $\mu$ -FID designed in this work was also compared with that of a commercial FID. For comparison, the analog signals from the commercial FID were recorded by the same recorder as that of the  $\mu$ -FID, *i.e.*, N2000 chromatographic station. The two detectors were operated under their own optimized conditions and their signals were recorded at the same frequency. A standard sample of n-hexadecane was used for testing the sensitivity of FIDs. The standard sample was diluted to a concentration of 1.0 mg/l in isoctane. The injection volume was 0.1  $\mu$ l. The results of comparative study were presented in Table 3. The signal-to-noise ratio of the  $\mu$ -FID was about 3 times as that of the commercial FID being tested.

## 5. Conclusion

In this work, a miniaturized  $\mu$ -FID was designed and developed with conventional mechanical fabrication techniques. Some general structure characters of conventional FID were changed to achieve simplification and better performances. Based on this design, the  $\mu$ -FID could work under high polarization voltage, which yielded a higher signal-to-noise ratio and sensitivity than conventional FID. Moreover, the consumption of gas was only one-third of that required for conventional FID, and only hydrogen gas and air were necessary for proper operation. The reduction of gas and power consumption is a significant merit for cost and energy saving. These characteristics of the  $\mu$ -FID make it very suitable for portable GC in field or *in situ* applications.

## Acknowledgements

This work was supported by the National Natural Science Foundation of China (Grant No. 20627006), the High Tech Program from the Ministry of Science & Technology of China (Grant No. 2007AA06Z419) and Research Grant from the Chinese Academy of Sciences (Grant No. KJXC2-YW-H18).

## References

- [1] G.A. Eiceman, H.H. Hill, J. Gardea-Torresdey, *Anal. Chem.* 70 (1998) 321R–339R.
- [2] G.A. Eiceman, J. Gardea-Torresdey, E. Overton, K. Carney, F. Dorman, *Anal. Chem.* 74 (2002) 2771–2780.
- [3] G. Etiope, *J. Chromatogr. A* 775 (1997) 243–249.
- [4] C. Ionel, C. Adrian, *J. Sep. Sci.* 25 (2002) 447–452.
- [5] J.A. Dziuban, M. Szczygielska, M. Malachowski, *Sens. Actuators A* 115 (2004) 318–330.
- [6] A.J. Grall, R.D. Sacks, *Anal. Chem.* 71 (1999) 5199–5205.
- [7] H. Smith, E.T. Zellers, R. Sacks, *Anal. Chem.* 71 (1999) 1610–1616.
- [8] C.-J. Lu, J. Whiting, R.D. Sacks, E.T. Zellers, *Anal. Chem.* 75 (2003) 1400–1409.
- [9] P.R. Lewis, R.P. Manginell, D.R. Adkins, R.J. Kottenstette, D.R. Wheeler, S.S. Sokolowski, D.E. Trudell, J.E. Byrnes, M. Okandan, J.M. Bauer, R.G. Manley, G.C. Frye-Mason, *IEEE Sens. J.* 6 (2006) 784–795.
- [10] E.J. Staples, S. Viswanathan, *Ind. Eng. Chem. Res.* 47 (2008) 8361–8367.
- [11] H.H. Hill, G.D. McMinn, *Detector for Capillary Chromatograph*, Wiley, New York, 1992.
- [12] S. Zimmermann, S. Wischhusen, J. Muller, *Sens. Actuators B* 63 (2000) 159–166.
- [13] S. Zimmermann, P. Krippner, A. Vogel, J. Muller, *Sens. Actuators B* 83 (2002) 285–289.
- [14] K.B. Thurbide, C.D. Anderson, *Analyst* 128 (2003) 616–622.
- [15] K.B. Thurbide, T.C. Hayward, *Anal. Chim. Acta* 519 (2004) 121–128.
- [16] T.C. Hayward, K.B. Thurbide, *Talanta* 73 (2007) 583–588.
- [17] P.L. Patterson, *J. Chromatogr. Sci.* 24 (1986).
- [18] T. Holm, *J. Chromatogr. A* 842 (1999) 221–227.
- [19] T. Holm, J.Φ. Madsen, *Anal. Chem.* 68 (1996) 3607–3611.